Available online at www.sciencedirect.com
ScienceDirect
JOURNAL OF RARE EARTHS
www.re-journal.com/en/
ELSEVIER
JOURNAL OF RARE EARTHS, Vol. 34, No. 10, Oct. 2016, P. 1048

Crystal-field analyses for trivalent lanthanide ions in $LiYF_4$

CHENG Jun (程 军)[1], WEN Jun (闻 军)[2], CHEN Yonghu (陈永虎)[1], YIN Min (尹 民)[1], DUAN Changkui (段昌奎)[1,*]

(1. Key Laboratory of Strongly-Coupled Quantum Matter Physics, Chinese Academy of Sciences, School of Physical Sciences, University of Science and Technology of China, Hefei 230026, China; 2. School of Physics and Electronic Engineering, Anqing Normal University, Anqing 246011, China)

Received 11 March 2016; revised 8 April 2016

Abstract: Based on the completely parametric crystal-field model, the energy level parameters, including free-ion parameters and crystal-field parameters, obtained by fitting the experimental energy level data sets of Ln^{3+} in $LiYF_4$ were systematically analyzed. The results revealed that the regular variation trends of the major parameters at relatively low site symmetry still existed. The *g* factors of ground states were calculated using the parameters obtained from least-squares fitting. The results for Ce^{3+}, Nd^{3+}, Sm^{3+}, Dy^{3+} and Yb^{3+} were in good agreement with experiment, while those of Er^{3+} deviated from experiment dramatically. Further study showed that the *g* factors depended strongly on B^6_4, and a slightly different B^6_4 value of −580 cm^{-1} led to *g* factors agreeing well with the experimental values.

Keywords: crystal-field interactions; $LiYF_4$; lanthanide ions; variation trends; *g* factors; rare earths

The energy level parameters of trivalent lanthanide (Ln^{3+}) ions in hosts can be determined by least-squares fitting to the experimental energy level data sets[1–3]. Previous results on the energy level parameters of all Ln^{3+} in $Cs_2NaLnCl_6$[4] with high site symmetry show that the major parameters vary smoothly across the Ln^{3+} series. If the trend holds for Ln^{3+} in all hosts, especially for those with low site symmetry, then it can be used to predict the crystal-field parameters (CFPs) for all Ln^{3+} from those for one particular Ln^{3+} ion in the same host. In particular, the CFPs of Ce^{3+} in crystals can be calculated from *ab-initio* calculations[5–7].

Ln^{3+} doped luminescent materials are widely applied as phosphors, scintillators, laser materials and temperature sensors[8–13]. Among these, Ln^{3+} doped $LiYF_4$ crystal has been deeply investigated with many spectroscopic and theoretical studies in the last several decades[14–17]. Hence, we chose Ln^{3+} in $LiYF_4$ to study the variation trends of energy level parameters, especially for crystal-field (CF) interactions, for a low site symmetry case.

The $LiYF_4$ crystal has the scheelite structure. Ln^{3+} ion occupies Y^{3+} site at S_4 point symmetry, surrounded by a slightly distorted dodecahedron of eight F^- ions. As the distortion is very small, D_{2d} symmetry is chosen as a realistic approximation to the actual S_4 site symmetry[18–20]. In D_{2d} symmetry, all the CFPs are real. Firstly, the energy level parameters of Ln^{3+} series in $LiYF_4$ were calculated from least-squares fitting to the experimental energy level data sets. Based on the fitted parameters, the *g* factors of the ground states of Ln^{3+} were analyzed. The results for Ce^{3+}, Nd^{3+}, Sm^{3+}, Dy^{3+} and Yb^{3+} were in good agreement with the experimental data, while those of Er^{3+} deviated from the experimental data. Further study showed that the *g* factors of Er^{3+} were sensitive to B^4_6 value in a particular range, and a slightly different value of B^6_4= −580 cm^{-1} could predict correct *g* factors.

1 Theoretical calculations

The energy levels of $4f^N$ configuration of Ln^{3+} in $LiYF_4$ were analyzed in terms of a completely parametric effective operator Hamiltonian:

$$H = E_{av} + \sum_k F^k f_k + \sum_i \zeta_f s_i \cdot l_i + \alpha L(L+1) + \beta G(G_2) + \gamma G(R_7) + \sum_h T^h t_h + \sum_s M^s m_s + \sum_k P^k p_k + H_{CF} \quad (1)$$

where all the parameters and operators have the same meaning as those in Ref. [21]. Specifically, E_{av} adjusts the configuration barycenter energy of the entire 4f*N* configuration. F^k (*k*=2, 4, 6) are the Slater parameters and f_k represent the angular operator parts of the electrostatic interaction. ζ_f is the spin-orbit parameters and $s_i \cdot l_i$ represent the spin-orbit interactions. *α*, *β*, and *γ* are the parameters describing the two-body interactions. *L* is the total orbital angular momentum, and $G(G_2)$ and $G(R_7)$ are Casimir operators for the groups G_2 and R_7. For $4f_N$ and 4f14-*N* configurations of $N \geq 3$, the three-body parameters T^h (*h*=2, 3, 4, 6, 7, 8) and corresponding operators t_h are employed. M^s (*s*=0, 2, 4) are the Marvin inte-

Foundation item: Project supported by the National Key Basic Research Program of China (2013CB921800), the National Natural Science Foundation of China (11274299, 11374291, 11574298, 11204292, 11404321) and the Anhui Provincial Natural Science Foundation (1308085QE75)

* **Corresponding author:** DUAN Changkui (**E-mail:** ckduan@ustc.edu.cn; **Tel.:** +86-551-63606287)

DOI: 10.1016/S1002-0721(16)60133-3

grals which describe the spin-spin and spin-other-orbit relativistic interactions between electrons. P^k (k=2, 4, 6) describe the two-body magnetic interactions. HCF is the CF Hamiltonian comprising the non-spherically symmetric crystal field.

In order to minimize the number of parameters in fitting the experimental data sets, M^2 and M^4 were constrained by the ratios M^2=0.56M^0, M^4=0.38M^0, and P^4 and P^6 were constrained by the ratios P^4=0.75P^2, P^6= 0.5P^2 [22,23].

The CF Hamiltonian H_{CF} for D_{2d} symmetry can be written (in the formalism of Wybourne) as[24]

$$H_{CF} = \sum_{k,q} B_q^k C_q^k = B_0^2 C_0^2 + B_0^4 C_0^4 + B_4^4 \left(C_4^4 + C_{-4}^4 \right) + B_0^6 C_0^6 + B_4^6 \left(C_4^6 + C_{-4}^6 \right) \quad (2)$$

where C_q^k is a spherical tensor of rank k, with components q; B_q^k are the CFPs.

Based on the effective Hamiltonian, least-squares fitting to the experimental energy levels available was performed to obtain the energy level parameters across the Ln^{3+} series in $LiYF_4$ using the f-shell program package[25]. Moreover, the magnetic properties were investigated. In the presence of an external magnetic field B, the Zeeman term can be written as[26]

$$\hat{H}_Z = \mu_B \left(g_s s + l \right) \cdot B \quad (3)$$

where μ_B is the Bohr magneton, g_s=2.00232 is the electron spin g factor, s and l are the spin and orbital angular momentum, respectively.

2 Results and discussion

The experimental energy level data sets of Ln^{3+} series in $LiYF_4$[20,24,27–35] except Pm^{3+} and Gd^{3+} were systematically analyzed by least-squares fitting using the parametric effective Hamiltonian. The Gd^{3+} in $LiYF_4$ was not included due to lack of energy level data at low excited states[36]. A summary of the calculated energy level parameters are presented in Table 1. Because of the limited amount of experimental data, some free-ion parameters were fixed using the values in Ref. [23]. The number of parameters (N_p) employed to fit the N_e energy levels is given in each case.

As can been seen, the Slater parameters F^k and the spin-orbit parameters ζ_{4f} have a regular increase across the Ln^{3+} series, which can be described by linear or second-order polynomial relation. The variation equations are as follows:

$$F^2=(63453\pm1016)+(3137.7\pm126.1)N \quad (4)$$

$$F^4=(46898\pm757)+(1993.4\pm94.0)N \quad (5)$$

$$F^6=(29965\pm1099)+(1960.0\pm136.4)N \quad (6)$$

$$\zeta_{4f}=(558.6\pm13.4)+(83.03\pm4.40)N+(7.443\pm0.310)N^2 \quad (7)$$

The variation trends of CFPs of Ln^{3+} in $LiYF_4$ were not as regular as those in Cs_2NaLnF_6, but smooth variations were presented by linear fitting to CFPs across the Ln^{3+} series, as shown in Fig. 1(a). The CF strength parameter S is a quantitative measure of the overall CF interaction of Ln^{3+} within a particular host and is defined as[37]

Table 1 Energy level parameters (in cm^{-1}) from fitting the $4f^N$ energy levels of Ln^{3+} series in $LiYF_4$[a,b]

Ln^{3+}	Ce	Pr	Nd	Sm	Eu	Tb	Dy	Ho	Er	Tm	Yb
E_{avg}	1513	10202	24412	47597	63642	69519	55344	48159	35753	18004	4632
F^2		68955	72952	79515	82573	90972	90421	93512	97326	101938	
F^4		50505	52681	56766	59646	(64499)	(63928)	66084	67987	71553	
F^6		33098	35476	40078	43203	(45759)	(46657)	49765	53651	51359	
ζ_{4f}	630	748	877	1168	1329	1702	1895	2126	2377	2632	2916
α		23.3	21.0	[20.5]	21.6	[17.6]	[17.9]	[17.2]	18.1	[17.3]	
β		[−644]	−579	[−616]	−482	[−581]	[−628]	[−596]	−599	[−665]	
γ		[1413]	1446	[1565]	1140	[1792]	[1790]	[1839]	1870	[1936]	
T^2			210	[282]	[370]	[330]	[326]	[365]	380		
T^3			41	[26]	[40]	[40]	[23]	[37]	41		
T^4			74	[71]	[40]	[45]	[83]	[95]	69		
T^6			−293	[−257]	[−300]	[−365]	[−294]	[−274]	−356		
T^7			321	[314]	[380]	[320]	[403]	[331]	239		
T^8			205	[328]	[370]	[349]	[340]	[343]	390		
M^0		[1.88]	[1.85]	[2.38]	2.41	[2.70]	[4.46]	3.92	4.41	[4.93]	
P^2		[244]	304	[336]	332	[482]	[610]	[582]	795	[730]	
B_0^2(ff)	354	512	391	370	339	413	360	386	325	339	446
B_0^4(ff)	[−1043]	−1127	−1031	−757	−733	−867	−737	−629	−749	−627	−560
B_4^4(ff)	[−1249]	−1239	−1271	−941	−1067	−1114	−943	−841	−1014	−913	−843
B_0^6(ff)	[−65]	−85	−28	−67	−36	−41	−35	−33	−19	−39	[−23]
B_4^6(ff)	[−1069]	−1205	−1046	−895	−764	−736	[−700]	−687	−635	−584	[−512]
σ	21.9	21.7	23.5	11.2	20.1	16.4	9.3	4.3	12.0	13.8	48.8
N_e	5	44	149	55	103	28	21	69	108	41	7
N_p	3	11	20	10	15	8	7	11	21	10	5

[a] Values in brackets were fixed according to Ref. [23]; for Ce^{3+} and Yb^{3+}, values were fixed according to variation trends; [b] Values in parentheses were constrained according to Ref. [23]: for Tb^{3+}, F^4/F^2=0.709, F^6/F^2=0.503; for Dy^{3+}, F^4/F^2=0.707, F^6/F^2=0.516

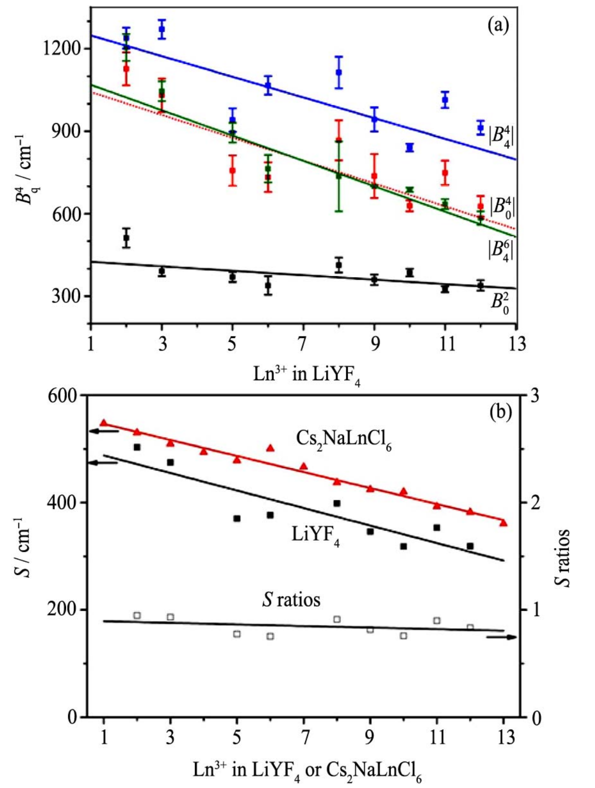

Fig. 1 (a) Variation trends of CFPs by fitting experimental energy levels of Ln^{3+} in $LiYF_4$; (b) *S* and *S* ratios of Ln^{3+} in $LiYF_4$ and $Cs_2NaLnCl_6$

$$S = \left(\frac{1}{3}\sum_k S_k^2\right)^{1/2}, \quad S_k^2 = \frac{1}{2k+1}\sum_{q=-k}^{k}\left|B_q^k\right|^2 \qquad (8)$$

Based on the calculated CFPs, CF strength parameters were analyzed, as shown in Fig. 1(b), together with *S* ratios of $LiYF_4$ and Cs_2NaLnF_6. The *S* ratios in two hosts can be considered as a constant (0.909) across the Ln^{3+} series.

The equations of CFPs and CF strength parameters described by linear relation were also given as follows:

B_0^2=(432.9±17.7)–(8.1±1.9)N (9)

B_0^4=(–1084.4±45.2)+(41.6±4.8)N (10)

B_4^4=(–1286.4±28.5)+(37.6±3.1)N (11)

B_0^6=(–68.4±14.0)+(3.5±1.7)N (12)

B_4^6=(–1115.2±27.6)+(46.1±3.1)N (13)

S(LYF)=(504.1±25.8)–(16.3±3.2)N (14)

$S(Cs_2NaLnCl_6)$=(561.5±6.3)–(14.9±0.8)N (15)

S(LYF)/$S(Cs_2NaLnCl_6)$=0.901±0.063 (16)

Note that the parameters of Ce^{3+} and Yb^{3+} were not included in the linear fitting of CFPs due to the limited experimental energy levels. The parameters of Ce^{3+} and Yb^{3+} were latter fitted using five and seven available experimental energy levels, respectively. Some parameters are poorly defined with the available experimental energy level data sets, and so are fixed to the values of variation trends during energy level fitting. Table 2 presents the linear variation trends of CFPs for Ln^{3+} in $LiYF_4$.

Based on the calculated energy level parameters, some multiplets of Nd^{3+}, Sm^{3+} and Er^{3+} were analyzed to compare with the experimental data, as presented in Fig. 2. It shows that the splittings using the two sets of energy level parameters are both consistent with the corresponding experimental values.

Table 2 Linear variation trends of CFPs for Ln^{3+} in $LiYF_4$ (in cm^{-1})

Ln^{3+}	B_0^2(ff)	B_0^4(ff)	B_4^4(ff)	B_0^6(ff)	B_4^6(ff)
Ce	425	−1043	−1249	−65	−1069
Pr	417	−1001	−1211	−61	−1023
Nd	409	−960	−1174	−58	−977
Pm	401	−918	−1136	−54	−931
Sm	392	−876	−1098	−51	−885
Eu	384	−835	−1061	−47	−839
Gd	376	−793	−1023	−44	−793
Tb	368	−752	−986	−40	−746
Dy	360	−710	−948	−37	−700
Ho	352	−668	−910	−33	−654
Er	344	−627	−873	−30	−608
Tm	336	−585	−835	−26	−562
Yb	328	−544	−798	−23	−516

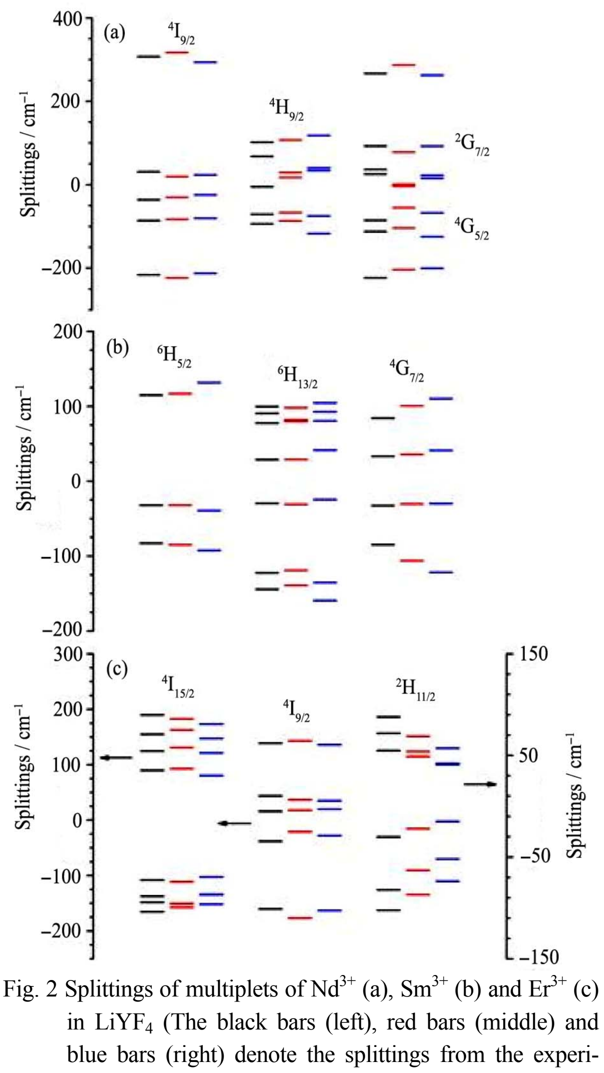

Fig. 2 Splittings of multiplets of Nd^{3+} (a), Sm^{3+} (b) and Er^{3+} (c) in $LiYF_4$ (The black bars (left), red bars (middle) and blue bars (right) denote the splittings from the experimental data, the fitted data and the calculated data using the trend values, respectively)

The values of CFPs for Ce^{3+} in $LiYF_4$ from *ab-initio* calculation[7] are B_0^2=310 cm^{-1}, B_0^4=−1104 cm^{-1}, B_4^4= −1418 cm^{-1}, B_0^6=−70 cm^{-1}, B_4^6=(−1140+237i) cm^{-1}, and the CF strength parameter is 520 cm^{-1}, merely 3.4% larger than that obtained using the CFPs from least-squares fitting. This indicates that, in a given host, the CFPs from *ab-initio* calculation for Ce^{3+} can be applied to predict the corresponding parameters and then the complicated energy level structures of other Ln^{3+} ions, where *ab-initio* calculations are computationally formidable.

Table 3 *g* factors of the ground states of Ln^{3+} in $LiYF_4$

Ln^{3+}	Ground states	g_z			g_x		
		Expt.[a]	Calc.[b]	Calc.[c]	Expt.[a]	Calc.[b]	Calc.[c]
Ce^{3+}	$^2F_{5/2}$	2.765	2.761	2.890	1.473	1.576	1.532
Nd^{3+}	$^4I_{9/2}$	1.987	1.550	1.488	2.554	2.674	2.671
Sm^{3+}	$^6H_{5/2}$	0.410	0.455	0.450	0.644	0.739	0.727
Dy^{3+}	$^6H_{15/2}$	1.112	0.899	0.568	9.219	9.168	9.135
Er^{3+}	$^4I_{15/2}$	3.137	8.452	4.974	8.105	4.376	7.524
Yb^{3+}	$^2F_{7/2}$	1.331	1.338	1.310	3.917	3.978	3.980

[a] Experimental values from Refs. [20, 38, 39]; [b,c] Values calculated using the sets of Slater parameters, spin-orbit parameters and CFPs from least- squares fitting and variation trends, respectively

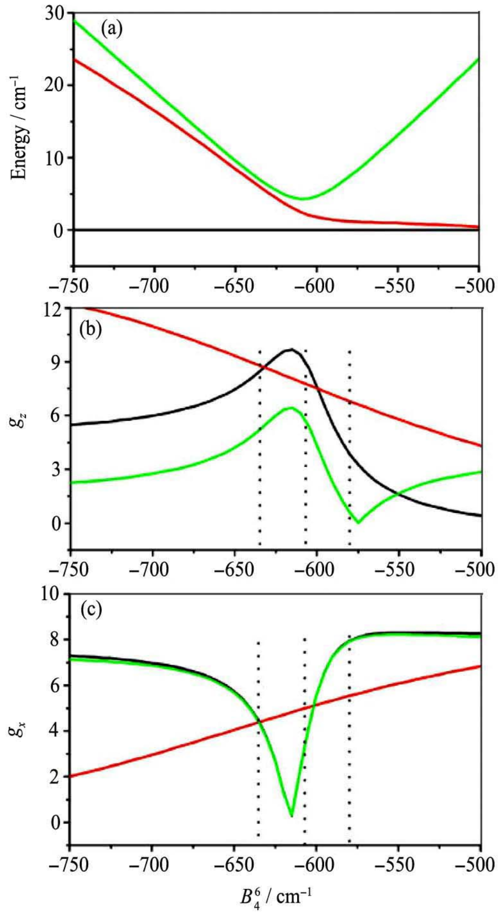

Fig. 3 Variation curves of the position of the lowest three Kramers doublets (black, red and green lines) (a) and corresponding g_z (b) and g_x (c) of Er^{3+} with B_4^6 varying from −800 to −500 cm^{-1} (The values of B_4^6 marked at −635, −608 and −580 cm^{-1} (dotted vertical bars) are from energy level fitting, variation trends and a different value for *g* factors)

The magnetic properties were then investigated using the calculated parameters from both least-squares fitting and variation trends. Table 3 presents the calculated *g* factors of the ground states of Ln^{3+} in $LiYF_4$. The results for Ce^{3+}, Nd^{3+}, Sm^{3+}, Dy^{3+} and Yb^{3+} are in good agreement with experimental values, while those for Er^{3+} deviate from the experimental data. We found that the energies of the first few levels and the *g* factors are sensitive to the value of B_4^6 in a particular range, but not so sensitive to other CFPs. Fig. 3 presents the variations of the position of the lowest three Kramers doublets and the corresponding g_z and g_x of Er^{3+} with B_4^6 value varying from −800 to −500 cm^{-1}. The *g* factors are closer to the experimental values when the strength of B_4^6 decreases, in accord with the variation trends. Optimized values B_4^6= −580 cm^{-1} and B_0^2=344 cm^{-1} predict g_z=3.062 and g_x= 8.037, agreeing well with experiment.

3 Conclusions

The energy level parameters were analyzed by fitting the experimental energy level data sets across the Ln^{3+} series in $LiYF_4$. The linear or second-order polynomial fitting of the parameters to the number of 4f electrons were performed. To some extent, the regular variation trends of the major parameters for a low symmetry site were maintained. Since CFPs of Ce^{3+} in a given host could be calculated from *ab-initio* calculation, the CFPS of other Ln^{3+} ions could be obtained by following the trends, so that the energy levels of all Ln^{3+} ions in the same host could be calculated. Based on the CF analyses, the *g* factors of the ground states of Ln^{3+} in $LiYF_4$ were also analyzed. The results for Ce^{3+}, Nd^{3+}, Sm^{3+}, Dy^{3+} and Yb^{3+} were in good agreement with the experimental data, while those of Er^{3+} deviated from the experimental data. Further study showed that the *g* factors of Er^{3+} were sensitive to B_4^6 value, and a slightly different value of B_4^6 =−580 cm^{-1} could predict correct *g* factors. This suggests that *g* factors can be taken into account to check or to increase the reliability of CFPs.

References:

[1] Tanner P A, Kumar V V R K, Jayasankar C K, Reid M F. Analysis of spectral data and comparative energy level parametrizations for Ln^{3+} in cubic elpasolite crystals. *J. Alloys Compd.*, 1994, **215**(1-2): 349.

[2] Quagliano J R, Richardson F S, Reid M F. Comparative analyses of Nd^{3+} ($4f^3$) energy level structures in various crystalline hosts. *J. Alloys Compd.*, 1992, **180**(1-2): 131.

[3] Wensky D A, Moulton W G. Energy levels of Pr^{3+} in various crystal hosts. *J. Chem. Phys.*, 1970, **53**(10): 3957.

[4] Duan C K, Tanner P A. What use are crystal field parameters? A chemist's viewpoint. *J. Phys. Chem. A*, 2010, **114**(19): 6055.

[5] Reid M F, Duan C K, Zhou H W. Crystal-field parameters form *ab initio* calculations. *J. Alloys Compd.*, 2009, **488**(2):

591.

[6] Hu L S, Reid M F, Duan C K, Xia S D, Yin M. Extraction of crystal-field parameters for lanthanide ions from quantum-chemical calculations. *J. Phys.: Condens. Matter*, 2011, **23**(4): 045501.

[7] Wen J, Ning L X, Duan C K, Chen Y H, Zhang Y F, Yin M. A theoretical study on the structural and energy spectral properties of Ce^{3+} ions doped in various fluoride compounds. *J. Phys. Chem. C*, 2012, **116**(38): 20513.

[8] Jiao H Y, Wang Y H. $Ca_2Al_2SiO_7$:Ce^{3+},Tb^{3+}: a white-light phosphor suitable for white-light-emitting diodes. *J. Electro. Chem. Soc.*, 2009, **156**(5): J117.

[9] Wang Y H, Zhu G, Xin S Y, Wang Q, Li Y Y, Wu Q S, Wang C, Wang X C, Ding X, Geng W Y. Recent development in rare earth doped phosphors for white light emitting diodes. *J. Rare Earths*, 2015, **33**(1): 1.

[10] Liu L S, Chen H H, Liu B Q, Zhang H, Tang B, Feng X J, Sun Z J, Zhao J T. Synthesis, structure and luminescent properties of a new Vernier phase $Lu_7O_6F_9$ doped by Eu^{3+} as potential scintillator with unique lath tube architecture. *J. Rare Earths*, 2014, **32**(8): 686.

[11] Okada F, Togawa S, Ohta K, Koda S. Solid-state ultraviolet tunable laser: a Ce^{3+} doped $LiYF_4$ crystal. *J. Appl. Phys.*, 1994, **75**: 49.

[12] Wu H, Yuan F F, Sun S J, Huang Y S, Zhang L Z, Lin Z B, Wang G F. Growth and spectral characteristics of a new promising stoichiometric laser crystal: $Ca_9Yb(VO_4)_7$. *J. Rare Earths*, 2015, **33**(3): 239.

[13] Zhou S S, Deng K M, Wei X T, Jiang G C, Duan C K, Chen Y H, Yin M. Upconversion luminescence of $NaYF_4$:Yb^{3+},Er^{3+} for temperature sensing. *Opt. Commun.*, 2013, **291**: 138.

[14] van Pieterson L, Reid M F, Wegh R T, Soverna S, Meijerink A. $4f^n \rightarrow 4f^{n-1}5d$ transitions of the light lanthanides: experiment and theory. *Phys. Rev. B*, 2002, **65**(4): 045113.

[15] van Pieterson L, Reid M F, Burdick G W, Meijerink A. $4f^n \rightarrow 4f^{n-1}5d$ transitions of the heavy lanthanides: experiment and theory. *Phys. Rev. B*, 2002, **65**(4): 045114.

[16] Rudowicz C, Qin J. Trends in the crystal (ligand) field parameters and the associated conserved quantities for trivalent rare-earth ions at S_4 symmetry sites in $LiYF_4$. *J. Alloys Compd.*, 2004, **385**(1-2): 238.

[17] Ogasawara K, Watanabe S, Toyoshima H, Ishii T, Brik M G, Ikeno H, Tanaka I. Optical spectra of trivalent lanthanides in $LiYF_4$ crystal. *J. Solid State Chem.*, 2005, **178**(2): 412.

[18] Jessen H P, Linz A, Leavitt R P, Morrison C A, Wortman D E. Analysis of the optical spectrum of Tm^{3+} in $LiYF_4$. *Phys. Rev. B*, 1975, **11**(1): 92.

[19] Christensen H P. Spectroscopic analysis of $LiHoF_4$ and $LiErF_4$. *Phys. Rev. B*, 1979, **19**(12): 6564.

[20] Wells J P R, Yamaga M, Han T P J, Gallagher H G, Honda M. Polarized laser excitation, electron paramagnetic resonance, and crystal-field analyses of Sm^{3+}-doped $LiYF_4$. *Phys. Rev. B*, 1999, **60**(6): 3849.

[21] Liu G K. Spectroscopic Properties of Rare Earth in Optical Materials. Edited by Liu G K, Jacquier B. Berlin: Springer, 2005. 1.

[22] Jayasankar C K, Reid M F, Richardson F S. Comparative crystal-field analyses of $4f^N$ energy levels in $LiYF_4$:Ln^{3+} systems. *Phys. Stat. Sol. B*, 1989, **155**(2): 559.

[23] Görller-Walrand C, Binnemans K. Handbook on the Physics and Chemistry of Rare Earths. Edited by Gschneidner K A, Jr., Eyring L. Amsterdam: Elsevier Science B.V., 1996, **23**: 121.

[24] dos Santos M A C, Antic-Fidancev E, Gesland J Y, Krupa J C, Lemaître-Blaise M, Porcher P. Absorption and fluorescence of Er^{3+}-doped $LiYF_4$: measurements and simulation. *J. Alloys Compd.*, 1998, **275**: 435.

[25] Reid M F. F-shell empirical programs. University of Canterbury, Christchurch, New Zealand, 1981.

[26] Abragam A, Bleaney B. Electron paramagnetic resonance of transition ions. New York: Dover Publications, Inc., 1986. 584.

[27] Peijzel P S, Vergeer P, Meijerink A, Reid M F, Boatner L A, Burdick G W. $4f^{n-1}5d \rightarrow 4f^n$ emission of Ce^{3+}, Pr^{3+}, Nd^{3+}, Er^{3+}, and Tm^{3+} in $LiYF_4$ and YPO_4. *Phys. Rev. B*, 2005, **71**(4): 045116.

[28] Wortman D E, Morrison C A, Leavitt R P. Energy levels and line intensities of Pr^{3+} in $LiYF_4$. *Phys. Rev. B*, 1979, **19**(12): 6442.

[29] de Leebeeck H, Görller-Walrand C. The simulation of polarized absorption and magnetic circular dichroism in $LiYF_4$:Nd^{3+}. *J. Alloys Compd.*, 1998, **275**: 407.

[30] Görller-Walrand C, Binnemans K, Fluyt L. Crystal-field analysis of Eu^{3+} in $LiYF_4$. *J. Phys.: Condens. Matter*, 1993, **5**(44): 8359.

[31] Romanova I V, Egorov A V, Korableva S L, Malkin B Z, Tagirov M S. ^{19}F NMR study of $LiTbF_4$ single crystals. *International Conference on Resonances in Condensed Matter: Altshuler100*, 2011, **324**: 012034.

[32] Barnes N P, Allen R E. Room-temperature Dy-LYF laser operation at 4.34 μm. *IEEE J. Quantum Elect.*, 1991, **27**(2): 277.

[33] Walsh B M, Grew G W, Barnes N P. Energy levels and intensity parameters of Ho^{3+} ions in $GdLiF_4$, $YLiF_4$ and $LuLiF_4$. *J. Phys.: Condens. Matter*, 2005, **17**(48): 7643.

[34] Klimin S A, Pytalev D S, Popova M N, Malkin B Z, Vanyunin M V, Korableva S L. High-resolution optical spectroscopy of Tm^{3+} ions in $LiYF_4$: crystal-field energies, hyperfine and deformation splittings, and the isotopic structure. *Phys. Rev. B*, 2010, **81**(4): 045113.

[35] Uehara N, Ueda K, Kubota Y. Spectroscopic measurements of a high-concentration Yb^{3+}:$LiYF_4$ crystal. *Jpn. J. Appl. Phys.*, 1996, **35**(4B): L499.

[36] Wegh R T, Donker H, Meijerink A, Lamminmäki R J, Hölsä J. Vacuum-ultraviolet spectroscopy and quantum cutting for Gd^{3+} in $LiYF_4$. *Phys. Rev. B*, 1997, **56**(21): 13841.

[37] Chang N C, Gruber J B, Leavitt R P, Morrison C A. Optical spectra, energy levels, and crystal-field analysis of tripositive rare earth ions in Y_2O_3. I. Kramers ions in C_2 sites. *J. Chem. Phys.*, 1982, **76**(8): 3877.

[38] Yosida T, Yamaga M, Lee D, Han T P J, Gallagher H G, Henderson B. The electron spin resonance and optical spectra of Ce^{3+} in $LiYF_4$. *J. Phys.: Condens. Matter*, 1997, **9**(18): 3733.

[39] Sattler J P, Nemarich J. Electron-paramagnetic-resonance spectra of Nd^{3+}, Dy^{3+}, Er^{3+}, and Yb^{3+} in lithium yttrium fluoride. *Phys. Rev. B*, 1971, **4**(1): 1.